
Designing over uncertain outcomes with stochastic sampling Bayesian optimization

Peter D. Tonner

Statistical Engineering Division
National Institute of Standards and Technology
Gaithersburg, MD 20874
peter.tonner@nist.gov

Daniel V. Samarov

Statistical Engineering Division
National Institute of Standards and Technology
Gaithersburg, MD 20874
daniel.samarov@nist.gov

A. Gilad Kusne

Materials Measurement Science Division
National Institute of Standards and Technology
Gaithersburg, MD 20874
aaron.kusne@nist.gov

Abstract

Optimization is becoming increasingly common in scientific and engineering domains. Oftentimes, these problems involve various levels of stochasticity or uncertainty in generating proposed solutions. Therefore, optimization in these scenarios must consider this stochasticity to properly guide the design of future experiments. Here, we adapt Bayesian optimization to handle uncertain outcomes, proposing a new framework called stochastic sampling Bayesian optimization (SSBO). We show that the bounds on expected regret for an upper confidence bound search in SSBO resemble those of earlier Bayesian optimization approaches, with added penalties due to the stochastic generation of inputs. Additionally, we adapt existing batch optimization techniques to properly limit the myopic decision making that can arise when selecting multiple instances before feedback. Finally, we show that SSBO techniques properly optimize a set of standard optimization problems as well as an applied problem inspired by bioengineering.

1 Introduction

Engineering tasks and scientific studies often rely on rapid identification of an optimal prototype or experimental condition. For instance, designing genetic sequences to improve protein fitness [Romero et al., 2012]. Due to the commonly high costs of generating proposed solutions at each iteration and the complex shape of the objective being targeted, interest has been growing around the use of Bayesian optimization for these problems [Shahriari et al., 2016]. Bayesian optimization (BO) combines statistical modeling with a quantitative specification of an ideal search to rapidly identify best solutions and have been applied to diverse industrial and scientific endeavors including drug discovery [Pyzer-Knapp, 2018], aerospace engineering [Hebbal et al., 2019], and alloy design [Vellanki et al., 2017].

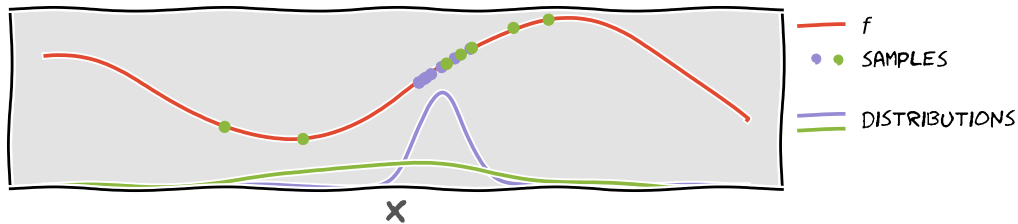


Figure 1: **Optimization under stochastic sampling** When sampling from an objective function f (red) stochastically, different sampling distributions must be considered (solid lines). The choice of distribution will impact both the maximum value of sampled observations as well as the variance of observed values.

Despite the widespread interest in applying BO to science and engineering, there remain issues with standard BO techniques limiting their impact. There are often real-world constraints that violate the assumptions in standard BO, and various methods have been developed to augment BO methods to address them [Vellanki et al., 2017, Azimi et al., 2010, Letham et al., 2018]. In this work we aim to handle cases where candidate solutions are not built exactly but instead are drawn from one of many sampling distributions (Fig. 1). We refer to this approach as *stochastic sampling* BO (SSBO).

Stochastic sampling occurs in many domains where iterative design and discovery are made. In synthetic biology, it is oftentimes too costly to synthesize individual genetic variants compared to generating large numbers of variants at once through a randomization process called mutagenesis [Kinney et al., 2010, Zheng et al., 2017]. Additionally, synthetic biology is a field with a growing interest in computer aided design [Wu et al., 2019]. In this work, we present a simulated design of function through promoters, which control the relative level of gene expression in bacteria and are a common target of synthetic biology design studies [Purnick and Weiss, 2009]. We focus on this application in this study, but we believe stochastic sampling is a common design constraint across engineering and science.

In this paper, we propose a solution to SSBO that takes the expectation of an upper confidence bound over each sampling distribution. We show that our proposed algorithm achieves bounds on regret comparable to standard BO techniques with an additional constant term corresponding to sampling from a distribution at each iteration. We then extend this approach to the situation where multiple samples from each distribution is desired. Finally, we test our SSBO procedure on synthetic objective functions and a simulated bioengineering problem.

2 Background

Gaussian processes Gaussian processes (GPs) are non-parametric models of functional data, where any finite number of function values are distributed as a multivariate normal distribution [Rasmussen and Williams, 2006]. Specifically, we obtain observations of an underlying process $f(x)$ through observations $y(x)$, possibly with observation noise. A GP is defined by a mean function $\mu(x)$ and covariance or kernel function $\kappa(x, x')$. The mean function is often assumed fixed ($\mu(x) = 0$) and the behavior of the GP is governed by the kernel. Kernels generally define an inner product between a (possibly infinite) feature space on x , and can be defined in a number of ways depending on the context [Hofmann et al., 2008]. In cases where observation noise is present a variance term σ_y^2 is included. Typically, $x \in \mathcal{R}^d$, although alternative domains are possible when supported by the kernel.

When trained on data \mathbf{x}, \mathbf{y} , the predictive mean and variance for a new observation y^* corresponding to point x^* are

$$\mu(x^*) = \kappa(x^*, \mathbf{x})(\kappa(\mathbf{x}, \mathbf{x}) + I\sigma_y^2)^{-1}\mathbf{y} \quad (1)$$

and

$$\sigma^2(x^*) = \kappa(x^*, x^*) - \kappa(x^*, \mathbf{x})(\kappa(\mathbf{x}, \mathbf{x}) + I\sigma_y^2)^{-1}\kappa(\mathbf{x}, x^*), \quad (2)$$

respectively. Here, each (x, y) pair corresponds to a candidate solution x and the function observation y .

Bayesian optimization The purpose of BO is to identify

$$x^* = \arg \max_{x \in D} f(x), \quad (3)$$

for some search space D and optimization target f [Shahriari et al., 2016, Snoek et al., 2012]. BO is particularly well suited to searches over large spaces of potential solutions, costly sampling procedures, and a target function $f(x)$ with many local optima. These techniques also often carry rigorously defined bounds on the distance from the global optimum at each iteration $r_t = f(x^*) - f(x_t)$, called the *regret* [Srinivas et al., 2012].

BO combines a statistical model, typically a GP, with a quantitative measure of the next desired observation, called the acquisition function. Srinivas et al. [2012] established provable regret bounds when BO is conducted with a GP as the function approximator and the upper confidence bound (UCB) as the acquisition function. UCB has the form

$$\alpha_t(x) = \mu_t(x) + \beta_t^{1/2} \cdot \sigma_t(x), \quad (4)$$

where μ_t and σ_t are the predictive mean and standard deviation of the GP at iteration t and β_t is a predefined, iteration-dependent value. Under mild assumptions of the GP kernel and f , selecting x_t from the maximum of the UCB leads to sub-linear cumulative regret ($R_T = \sum_{i=1}^T r_i$) with high probability (e.g. $\lim_{t \rightarrow \infty} \frac{R_T}{t} = 0$).

Batch Bayesian optimization While standard BO assumes that observations from the process $f(x)$ are generated one at a time (referred to as *sequential* optimization), there has been considerable effort to expand BO techniques to cases where more than one observation is made at each iteration. These techniques are referred to as *batch* Bayesian optimization [Kathuria et al., 2016, González et al., 2015, Desautels et al., 2014]. In order to avoid myopic over-exploitation, batch BO algorithms approximate the feedback that would be received if selection was performed in a sequential manner by modifying the acquisition function during batch construction.

Constrained BO Real-world applications often cannot map directly to the standard BO framework. This has led to many studies on the use of BO in the presence of constraints [Azimi et al., 2010, Letham et al., 2018]. Notable approaches are those which combine constraints on the optimization problem with stochastic selection of new candidates [Azimi et al., 2016, Yang et al., 2019]. In this work, we instead consider the expected reward given a sampling distribution directly, and establish provable regret bounds on BO performed in this manner.

3 Optimization via stochastic samples

We consider the problem of maximizing a function $f(x)$ when x is sampled from a distribution $\pi(x|\theta)$. Specifically the goal is to solve Eq. 3 by choosing sampling distribution parameters $\theta \in \Theta$ that minimize the expected regret with respect to the optimal $f(x^*)$

$$r_x(\theta) = E_{\pi(\theta)}[f(x^*) - f(x)] = f(x^*) - E_{\pi(\theta)}[f(x)], \quad (5)$$

where $E_{\pi(\theta)}$ is the expectation over the distribution $\pi(x|\theta)$. Given that the choice of θ impacts the regret only through the expectation of $f(x)$, we reframe the optimization in terms of the optimal sampling distribution θ^* :

$$\theta^* = \arg \min_{\theta \in \Theta} r_x(\theta) = \arg \max_{\theta \in \Theta} E_{\pi(\theta)}[f(x)]. \quad (6)$$

We also define the expected regret relative to the optimal θ^* for a chosen θ ,

$$r_\pi(\theta) = r_x(\theta) - r_x(\theta^*) \quad (7)$$

$$= E_{\pi(\theta^*)}[f(x)] - E_{\pi(\theta)}[f(x)]. \quad (8)$$

Given that $r_x(\theta^*)$ is fixed for a given f and Θ , minimizing r_x (and r_π) corresponds to maximizing the expectation of f over θ .

Our goal is to develop an iterative procedure where at each iteration t , we select θ_t to minimize our instantaneous regret $r_x(\theta)$. Ultimately, we aim to minimize the total regret at T rounds $R_T =$

```

Data: Sampling distribution  $\pi$ , parameter space  $\Theta$ , GP prior with  $\mu_0 = 0, \sigma_y^2, k$ 
for  $t = 1, 2, \dots$  do
  Define  $\alpha_t(x) = \mu_{t-1}(x) + \beta_t^{1/2} \sigma_{t-1}(x)$ ;
  Choose  $\theta_t = \arg \max_{\theta \in \Theta} E_{\pi(\theta)}[\alpha_t(x)]$ ;
  Sample  $x_t \sim \pi(\theta)$  and  $y_t = f(x_t) + \epsilon$ ;
  Update GP with data point  $(x_t, y_t)$ ;
end

```

Algorithm 1: Stochastic sampling GPUCB algorithm

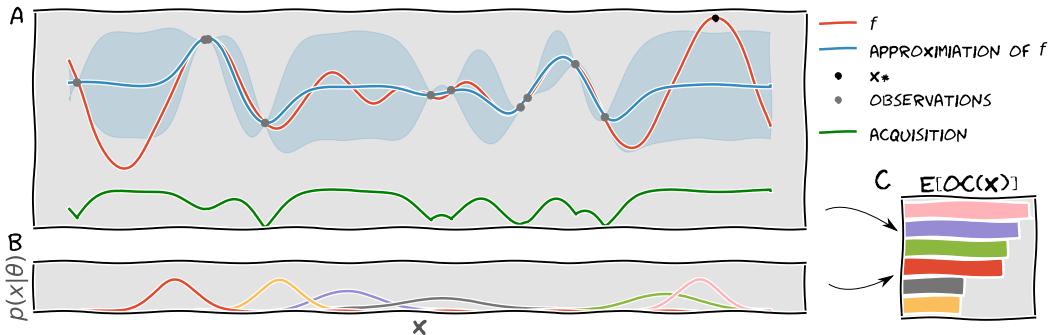


Figure 2: **Stochastic sampling Bayesian optimization.** (A) Observations (gray) of the function f (red) are used to construct a GP (blue, solid line is mean and shaded region is 95% confidence interval) and a standard BO acquisition function ($\alpha(x)$, green). (B) Different sampling distributions ($\pi(\theta)$) are available from which to generate new x samples. This example uses normal distributions with parameters $\theta = \{\mu, \sigma^2\}$. (C) The expectation of $\alpha(x)$ for various values of θ .

$\sum_{t=1}^T r_x(\theta_t)$. In order to identify the θ with minimal regret at iteration t , we adopt the UCB bound proposed in Eq. 4. Specifically, at each iteration t , we select θ_t with the maximal expected value of $\alpha_t(x)$:

$$\theta_t := \arg \max_{\theta \in \Theta} E_{\pi(\theta)}[\alpha_t(x)]. \quad (9)$$

The complete procedure, stochastic sampling GP-UCB (SS-GPUCB), can be seen in Algorithm 1 and Fig. 2. In the next section, we describe bounds on R_T for both discrete and continuous sampling distributions when iterative values of θ_t are selected using SS-GPUCB.

3.1 Bounding expected regret

The regret bounds established in this work build on those constructed for standard GP-UCB [Srinivas et al., 2012]. The regret bounds for SS-GPUCB include a term representing the maximal mutual information between T observations Y_T and the true function f , $\gamma_T = \max_{|A|=T, A \subset D} I(Y_A; f)$. We define an additional constant in this work, relating the regret bounds to the sampling distributions used for search. For sampling distributions $\pi(x|\theta)$, we define a constant

$$\pi^* := \max_{x \in D, \theta \in \Theta} \pi(x|\theta). \quad (10)$$

π^* corresponds to the maximal pdf value of π for all possible x and θ in the optimization problem. In order to ensure that π^* remains well defined, we assume that Θ is bounded. For example, in the case of a Gaussian distribution where $\theta = \{\mu, \sigma\}$, $\lim_{\sigma \rightarrow 0} \pi^* = \infty$. In this case, we would assume that Θ will be defined such that $\sigma > 0 \quad \forall \theta \in \Theta$. Using these terms, we now state the main theoretical results of this work.

For both discrete and continuous distributions, the bounds on the cumulative expected regret at iteration T are of the form

$$\mathcal{O}^*(\sqrt{T\beta_T\gamma_T\pi^*d}). \quad (11)$$

Here \mathcal{O}^* corresponds to a specialized form of the standard \mathcal{O} where logarithmic terms are removed and d is the size of the search space. Full proofs for these bounds are available in the appendix. These bounds are similar to that of Srinivas et al. [2012], with $\sqrt{\pi^* d}$ corresponding to an added impact of sampling from a distribution. These bounds maintain the sub-linear cumulative regret of standard GPUCB, enabling efficient optimization in stochastic sampling scenarios.

3.2 Optimizing over stochastic batch experiments

Experiments are often conducted generating multiple observations for a given set of experiment parameters, i.e. a given θ . In this case we wish to improve the selection of θ by considering the potential information shared between individual observations. To this end, we adopt techniques from batch BO [Desautels et al., 2014]. Our methods are similar to batch BO in that multiple observations will be collected in each feedback iteration. Our approach differs from these techniques, however, in the selection of a single θ value at each iteration from which many observations will be drawn. We distinguish our approach from other batch BO methods by referring to this as *stochastic* batch BO.

We adopt the technique of approximating the expected feedback that would be received during sequential search through a penalty applied on the acquisition function. This penalty, $\varphi(x_i; x_j)$, defines the approximate impact that observing $f(x_j)$ would have on $\alpha_t(x_i)$. It is a heuristic that acts as a local penalizer around x_j , meaning that it is differentiable, $0 \leq \varphi(x_i; x_j) \leq 1$, and $\varphi(x_i; x_j)$ is non-decreasing as the distance between x_i and x_j grows (see appendix for explicit form) [González et al., 2015].

Using a penalty term enforces exploration when selecting θ by decreasing $\alpha(x)$ around the positions most likely to be sampled for a given $\pi(\theta)$ (Fig. 3). As we show below, these methods enable independent marginalization of approximate acquisition values. While other methods of constructing batch samples exist for Bayesian optimization, they require combinatorial searches over the previously sampled batch values (see appendix). As such, we focus on heuristic approaches here.

At iteration t we will sample B new observations from the distribution $\pi(x|\theta_t)$. For each new point x_i ($1 \leq i \leq B$), given the previous observations in the batch $x_{1:i-1} = \{x_1, \dots, x_{i-1}\}$, the acquisition function for x_i is

$$\alpha_t(x_i) \cdot \prod_{j=1}^{i-1} \varphi(x_i; x_j). \quad (12)$$

The advantage of the formulation of batch acquisition values in Eq. 12 is that the acquisition can be easily marginalized for each observation x_i over previous observations $x_{1:i-1}$ (Fig. 3). Specifically, each element of $x_{1:i-1}$ is *iid* and so the expectation of the penalty is

$$E_{\pi(\theta)} \left[\prod_{j=1}^{i-1} \varphi(x_i; x_j) \right] = \prod_{j=1}^{i-1} E_{\pi(\theta)} \left[\varphi(x_i; x_j) \right] \quad (13)$$

$$= \prod_{j=1}^{i-1} \varphi_{\pi(\theta)}(x_i) = (\varphi_{\pi(\theta)}(x_i))^{i-1}, \quad (14)$$

where we introduce the function $\varphi_{\pi(\theta)}(x_i)$ representing the expected penalty over $\pi(\theta)$ (Fig. 3C). This then translates to calculating the expected acquisition value for each iteration i and ultimately for varying batch size B (Fig. 3E,F). We choose θ_t such that

$$\theta_t = \arg \max_{\theta \in \Theta} E_{\pi(\theta)} \left[\sum_{k=1}^B \alpha_t(x) \varphi_{\pi(\theta)}^{k-1}(x) \right]. \quad (15)$$

This approach, which we call stochastic batch GPUCB (SB-GPUCB), explicitly captures the trade-off between exploration and exploitation for varying batch size and sample distribution variance. Specifically, if batch size is small (e.g. approaching $B = 1$ for sequential search) then sampling distributions with smaller variance are preferred because they more precisely target the current maximum (Fig. 3F, purple bars). However, as batch size increases, broader sampling distributions are preferred in order to increase the information gained from multiple observations in a single

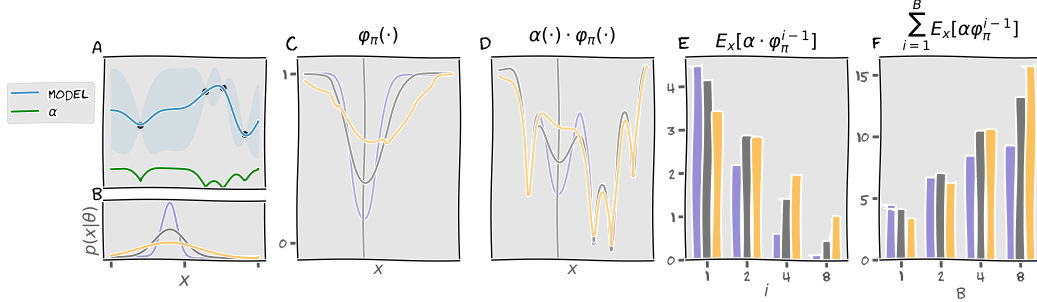


Figure 3: **Local penalization of the acquisition function over stochastic batches.** We display the effect of a locally penalized acquisition function for a model and acquisition function (A). Three sampling distributions, with the same mean and differing variances will be compared (B). The expected penalty φ_π is different for each distribution, due to differences in probability mass over x (C). This impacts the expected α differently for each distribution (D). Expectations for $\alpha(x)\varphi_\pi^{i-1}(x)$ decreases with i but for a different rate for each distribution (E). This leads to different optimal distributions depending on batch size (F, Eq. 15). x is removed from equations for simplicity.

```

Data: Sampling distribution  $\pi$ , parameter space  $\Theta$ , batch size  $B$ , GP prior with  $\mu_0 = 0, \sigma_y^2, k$ 
for  $t = 1, B, 2B, \dots$  do
    Define  $\alpha_t(x) = \mu_{t-1}(x) + \beta_t^{1/2} \sigma_{t-1}(x)$ ;
    Define  $\varphi_{\pi(\theta)} = E_{\pi(\theta)}[\varphi(\cdot; x)]$ ;
    Choose  $\theta_t = \arg \max_{\theta \in \Theta} E_{\pi(\theta)} \left[ \sum_{k=1}^B \alpha_t(x) \varphi_{\pi(\theta)}^{k-1}(x) \right]$ ;
    Sample  $x_j \sim \pi(\theta)$  and  $y_j = f(x_j) + \epsilon$  for  $t \leq j < t + B$ ;
    Update GP with data-points  $(x_j, y_j), t \leq j < t + B$ ;
end

```

Algorithm 2: Batch stochastic sampling GPUCB algorithm

batch (Fig. 3F, yellow bars). This effect is attenuated as the search begins to properly identify the function optimum, however (Fig. A.4). As the model becomes more complete, and therefore the acquisition value becomes a more accurate predictor of the function optimum, lower variance sampling distributions are preferred regardless of batch size. Therefore, the local penalty approach can properly adapt the selection of θ at each iteration to best take advantage of the provided batch size and current knowledge of the process f .

4 Experiments

Objective functions We selected objective functions from the optimization literature for evaluating our SSBO algorithms [Surjanovic and Bingham]. Details of these functions can be found in the appendix. They cover many useful characteristics when comparing optimization algorithms including many local optima, multiple periodicities and magnitudes, and sharp ridge boundaries.

Alternative acquisition functions We developed alternative acquisition functions to compare against our own procedure. We define the *maximum mean* acquisition as $E_{\pi(\theta)}[\mu_t(x)]$, which takes the expectation over $\pi(\theta)$ of the predictive mean and is a previously suggested exploitative strategy [Azimi et al., 2016]. *Mean GPUCB* is defined as $\alpha_t(E_{\pi(\theta)}[x])$ and corresponds to considering only the mean of the distribution $\pi(\theta)$. Finally, an *independent* model of α_t is used to test the impact of φ in batch sampling. The *independent* acquisition function is not relevant in sequential search because φ is not used. We also compare to *random* search, where all θ values are chosen uniformly at random.

Evaluating performance At iteration t , we consider both instantaneous regret:

$$r_t = f(x^*) - f(x_t), \quad (16)$$

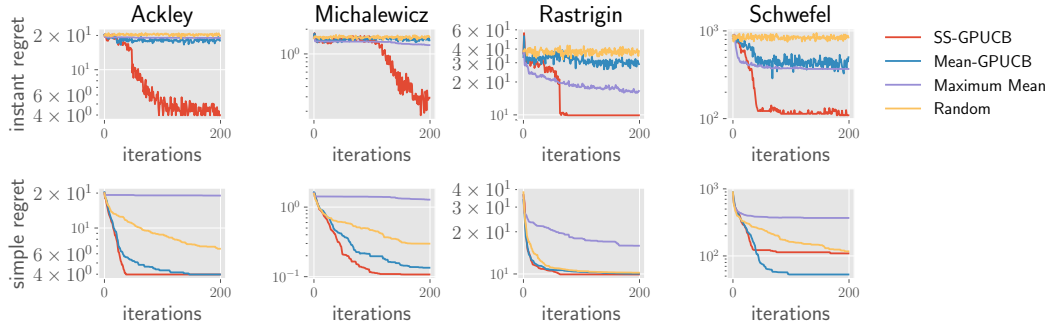


Figure 4: **Sequential SS-GPUCB regret.** For each acquisition function, we show the instantaneous regret (top, Eq. 16) and simple regret (bottom, Eq. 17) achieved under each objective.

and simple regret:

$$\min_{1 \leq i \leq t} r_t. \quad (17)$$

Each condition was run until a total of 200 observations was received and results were averaged over 50 simulations each.

Sampling distributions. Sampling distributions were constructed using a discretization of a normal distribution. Means were placed at 32 evenly spaced positions across both input dimensions, for a total of 1024 unique two-dimensional mean positions. Five standard deviations were chosen covering values from 10^{-3} to 2×10^{-1} the input dimension size.

Implementation Simulations were run in Python, using the GPy library for model inference [GPy, [since 2012](#)]. The source code for running the simulations is provided in the supplement.

4.1 Sequential stochastic optimization

We first tested SS-GPUCB under sequential feedback and compared it to other acquisition functions. We found that under both instantaneous and simple regret, SB-GPUCB outperformed all other methods, with one exception (Fig. 4). The one exception occurred when comparing SS-GPUCB to the Mean-GPUCB acquisition function under the Schwefel objective function. This difference appeared to be due to an early convergence to the local optima of that function in a small number of trials (Fig. A.2). Of particular note is the stark difference in performance of SS-GPUCB in instantaneous regret compared to the other methods considered. The other methods do not achieve considerable decrease in instantaneous regret over the course of the simulation, indicating that they do not properly combine the model predictions with the expected reward induced by different sampling distributions. This also likely indicates that gains in simple regret are due at least in part to the added random chance of improvement created by sampling x from a distribution $\pi(\theta)$.

4.2 Stochastic Batch optimization

We next considered the ability of SB-GPUCB to optimize functions under batch sampling. Again we found that compared to other acquisition functions, SB-GPUCB rapidly identifies optimal values of f (Fig. 5). This includes the comparison of a SB-GPUCB acquisition with no local penalty for batch observations (independent), which appears to lag considerably behind the locally penalized acquisition in minimizing regret. This indicates that approximating the change in α from each observation x_t using φ improves optimization over more naive methods.

Of particular interest is how the sampling distribution π is used in selecting the most optimal θ at each iteration. During sequential optimization, low variance distributions will be most advantageous because they allow for more precise selection of the next observation. However when observations are collected in batches, it is more useful to select high variance sampling distributions early in the search to more rapidly explore the input space. This behavior is directly reflected in the sampling variances selected by SS-GPUCB and SB-GPUCB under sequential and batch optimization, respectively (Fig.

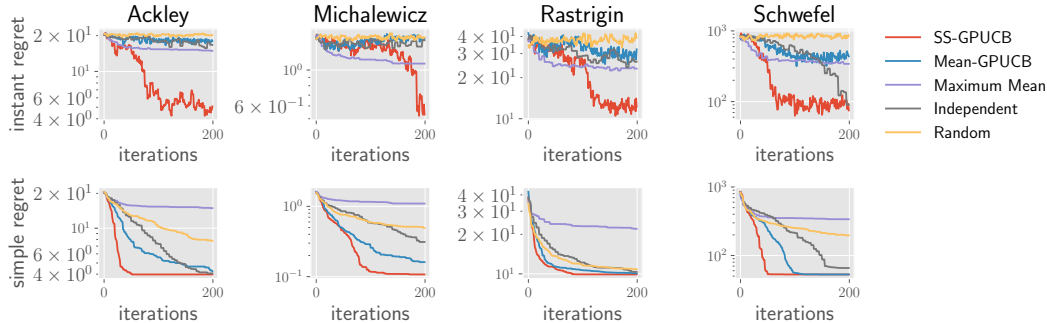


Figure 5: **Batch SS-GPUCB regret** Instantaneous and simple regret for each objective function under batch optimization with a batch size of 5.

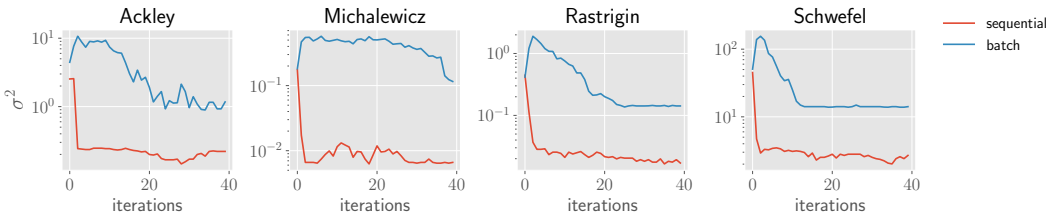


Figure 6: **Variance selection under sequential and batch optimization.** Variance of the distribution selected by SS-GPUCB (sequential, red) and SB-GPUCB (batch, blue) at each iteration.

6). In particular SS-GPUCB prefers low variance distributions throughout the simulation, with the exception of the first iteration where no data is available and all expectations of α for different values of θ are considered equal. We also see that initially SB-GPUCB selects higher variance early in the search and steadily declines over time. However, even during later iterations the variance selected during batch optimization does not converge to that selected during sequential optimization. This is due to the fact that the batch size remains constant over the simulation and an intermediate variance results in the highest expected return over the combination of all batch observations. We expect that if we adaptively selected the batch size, SB-GPUCB would choose the minimum variance in combination with a decreasing batch size as the model increasingly identifies the true optimum [Desautels et al., 2014].

4.3 Stochastic batch optimization of biological function

In order to validate our method for use in real world applications, we evaluated the performance of SB-GPUCB on a simulated problem in promoter design. Synthetic design of promoters is an ideal candidate for SSBO because the search space grows exponentially with the size of the genomic sequence and novel sequences are often generated through mutagenesis [Kinney et al., 2010, Currin et al., 2015]. Therefore, applying an upper confidence bound procedure to these tasks must consider the uncertainty inherent to the generation of new sequences. We considered a mutagenesis library design problem where five positions would be randomized with one of four mutation rates and every possible length five DNA sequence is used as a starting point for randomization (Fig. 7A,B). In this case, $\theta = \{s, \mu\}$ where $s \in \{A, C, T, G\}^5$ is the starting DNA sequence and μ is the mutation rate.

We developed a simulation of bacterial promoter design using a published model of the *Escherichia coli lac* promoter, which models the expression levels as a function of promoter sequence with linear and quadratic terms corresponding to individual nucleotide and position interactions, respectively [Otwinowski and Nemenman, 2013]. We use this published model as an oracle for simulating iterative design of the *lac* promoter at the regulatory targets of two proteins, CRP and RNAP. Each regulator targets two regions, which contained the largest linear and quadratic terms yielding a diverse fitness landscape on which to optimize (Figs A.7, A.8).

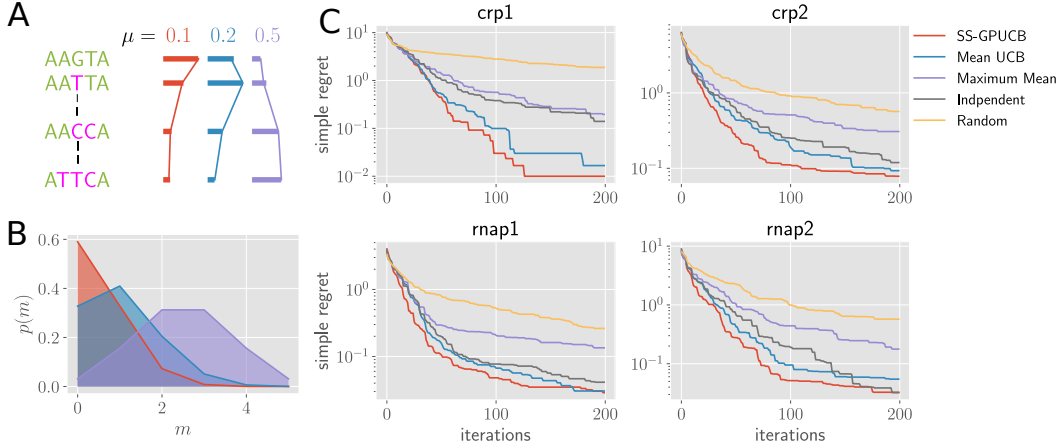


Figure 7: **Stochastic batch Bayesian optimization of the *lac* promoter.** (A) An initial DNA sequence (green) will be mutagenized with various mutation rates μ (red, blue, and purple). The probability of each mutation (pink letters) depends on the corresponding mutation rate (red, blue, and purple bars). (B) Probability of mutation numbers m for different mutation rates μ (same as in A). (C) Simple regret of each of the four regions of the *lac* promoter for each acquisition function.

Probabilistic modeling of sequence to phenotype is an active area of research [Riesselman et al., 2018]. We adapted a previous approach of modeling protein fitness with GPs and a linear kernel to predict the expression levels of the *lac* promoter as a function of the promoter sequence [Romero et al., 2012]. While relatively simple, we found that this model was able to capture relevant global trends in the data and would therefore provide a reasonable test of our algorithm’s performance (Fig. A.9), with the added advantage of providing a straight-forward GP model to use for SSBO.

We applied batch SS-GPUCB to each of the four *lac* promoter regions for each acquisition function for a batch size of five. We found that for each region, batch SS-GPUCB outperforms all other methods (Fig. 7C). We further expect that the difference in performance between batch SS-GPUCB and other methods would grow considerably as the size of each batch and sequence space are increased to reflect the sizes commonly seen in iterative genetic sequence design [Currin et al., 2015].

5 Conclusion

Stochastic sampling is common in scientific and engineering domains. We have provided the theoretical groundwork to enable broad application of BO techniques to optimization tasks with stochastic sampling, with proof of sub-linear regret bounds. Our empirical results suggest that this method will be successful in a broad range of applications, and enhance the use of BO in real-world optimization scenarios.

Acknowledgments

Funding for this project came from the NIST Innovation in Measurement Science Grant: Genetic Sensor Foundry for Predictive Engineering of Living Measurement Systems. PDT is additionally funded by the NRC Postdoctoral Fellowship. Analysis was performed on the NIST Enki HPC cluster. The identification of any commercial product or trade name does not imply endorsement or recommendation by the NIST, nor is it intended to imply that the materials or equipment identified are necessarily the best available for the purpose.

References

Javad Azimi, Xiaoli Fern, Alan Fern, Elizabeth Burrows, Frank Chaplen, Yanzhen Fan, Hong Liu, Jun Jaio, and Rebecca Schaller. Myopic policies for budgeted optimization with constrained experiments. In *Twenty-Fourth AAAI Conference on Artificial Intelligence*, 2010.

- Javad Azimi, Xiaoli Fern, and Alan Fern. Budgeted optimization with constrained experiments. *Journal of Artificial Intelligence Research*, 56(nil):119–152, 2016. doi: 10.1613/jair.4896. URL <https://doi.org/10.1613/jair.4896>.
- Andrew Currin, Neil Swainston, Philip J. Day, and Douglas B. Kell. Synthetic biology for the directed evolution of protein biocatalysts: Navigating sequence space intelligently. *Chemical Society Reviews*, 44(5):1172–1239, 2015. doi: 10.1039/c4cs00351a. URL <https://doi.org/10.1039/c4cs00351a>.
- Thomas Desautels, Andreas Krause, and Joel W. Burdick. Parallelizing exploration-exploitation tradeoffs in gaussian process bandit optimization. *Journal of Machine Learning Research*, 15: 4053–4103, 2014. URL <http://jmlr.org/papers/v15/desautels14a.html>.
- J. González, Z. Dai, P. Hennig, and N. D. Lawrence. Batch Bayesian Optimization via Local Penalization. *ArXiv e-prints*, May 2015. URL <http://adsabs.harvard.edu/abs/2015arXiv150508052G>.
- GPpy. GPpy: A gaussian process framework in python. <http://github.com/SheffieldML/GPpy>, since 2012.
- Ali Hebbal, Loïc Brevault, Mathieu Balesdent, El-Ghazali Talbi, and Nouredine Melab. Multi-objective optimization using deep gaussian processes: Application to aerospace vehicle design. In *AIAA Scitech 2019 Forum*, page 1973, 2019.
- Thomas Hofmann, Bernhard Schölkopf, and Alexander J. Smola. Kernel methods in machine learning. *The Annals of Statistics*, 36(3):1171–1220, 2008. doi: 10.1214/009053607000000677. URL <https://doi.org/10.1214/009053607000000677>.
- Tarun Kathuria, Amit Deshpande, and Pushmeet Kohli. Batched gaussian process bandit optimization via determinantal point processes. In D. D. Lee, M. Sugiyama, U. V. Luxburg, I. Guyon, and R. Garnett, editors, *Advances in Neural Information Processing Systems 29*, pages 4206–4214. Curran Associates, Inc., 2016. URL <http://papers.nips.cc/paper/6452-batched-gaussian-process-bandit-optimization-via-determinantal-point-processes.pdf>.
- J. B. Kinney, A. Murugan, C. G. Callan, and E. C. Cox. Using deep sequencing to characterize the biophysical mechanism of a transcriptional regulatory sequence. *Proceedings of the National Academy of Sciences*, 107(20):9158–9163, 2010. doi: 10.1073/pnas.1004290107. URL <https://doi.org/10.1073/pnas.1004290107>.
- Benjamin Letham, Brian Karrer, Guilherme Ottoni, and Eytan Bakshy. Constrained bayesian optimization with noisy experiments. *Bayesian Analysis*, nil(nil):nil, 2018. doi: 10.1214/18-ba1110. URL <https://doi.org/10.1214/18-ba1110>.
- Jakub Otwinowski and Ilya Nemenman. Genotype to phenotype mapping and the fitness landscape of the e. coli lac promoter. *PLoS ONE*, 8(5):e61570, 2013. doi: 10.1371/journal.pone.0061570. URL <https://doi.org/10.1371/journal.pone.0061570>.
- Priscilla E. M. Purnick and Ron Weiss. The second wave of synthetic biology: From modules to systems. *Nature Reviews Molecular Cell Biology*, 10(6):410–422, 2009. doi: 10.1038/nrm2698. URL <https://doi.org/10.1038/nrm2698>.
- E. O. Pyzer-Knapp. Bayesian optimization for accelerated drug discovery. *IBM Journal of Research and Development*, 62(6):2:1–2:7, 2018. doi: 10.1147/jrd.2018.2881731. URL <https://doi.org/10.1147/jrd.2018.2881731>.
- C.E. Rasmussen and C.K.I. Williams. *Gaussian Processes for Machine Learning*. Adaptive computation and machine learning series. University Press Group Limited, 2006. ISBN 9780262182539. URL <https://books.google.com/books?id=vWtwQgAACAAJ>.
- Adam J. Riesselman, John B. Ingraham, and Debora S. Marks. Deep generative models of genetic variation capture the effects of mutations. *Nature Methods*, 15(10):816–822, 2018. doi: 10.1038/s41592-018-0138-4. URL <https://doi.org/10.1038/s41592-018-0138-4>.

- P. A. Romero, A. Krause, and F. H. Arnold. Navigating the protein fitness landscape with gaussian processes. *Proceedings of the National Academy of Sciences*, 110(3):E193–E201, 2012. doi: 10.1073/pnas.1215251110. URL <https://doi.org/10.1073/pnas.1215251110>.
- Bobak Shahriari, Kevin Swersky, Ziyu Wang, Ryan P. Adams, and Nando de Freitas. Taking the human out of the loop: a review of bayesian optimization. *Proceedings of the IEEE*, 104(1): 148–175, 2016. doi: 10.1109/jproc.2015.2494218. URL <https://doi.org/10.1109/jproc.2015.2494218>.
- Jasper Snoek, Hugo Larochelle, and Ryan P. Adams. Practical bayesian optimization of machine learning algorithms. In *Proceedings of the 25th International Conference on Neural Information Processing Systems - Volume 2, NIPS'12*, pages 2951–2959, USA, 2012. Curran Associates Inc. URL <http://dl.acm.org/citation.cfm?id=2999325.2999464>.
- Ercan Solak, Roderick Murray-Smith, William E Leithead, Douglas J Leith, and Carl E Rasmussen. Derivative observations in gaussian process models of dynamic systems. In *Advances in neural information processing systems*, pages 1057–1064, 2003.
- Niranjan Srinivas, Andreas Krause, Sham M. Kakade, and Matthias W. Seeger. Information-theoretic regret bounds for gaussian process optimization in the bandit setting. *IEEE Transactions on Information Theory*, 58(5):3250–3265, 2012. doi: 10.1109/tit.2011.2182033. URL <https://doi.org/10.1109/tit.2011.2182033>.
- S. Surjanovic and D. Bingham. Virtual library of simulation experiments: Test functions and datasets. Retrieved May 2, 2019, from <http://www.sfu.ca/~ssurjano>.
- Pratibha Vellanki, Santu Rana, Sunil Gupta, David Rubin, Alessandra Sutti, Thomas Dorin, Murray Height, Paul Sanders, and Svetha Venkatesh. Process-constrained batch bayesian optimisation. In I. Guyon, U. V. Luxburg, S. Bengio, H. Wallach, R. Fergus, S. Vishwanathan, and R. Garnett, editors, *Advances in Neural Information Processing Systems 30*, pages 3414–3423. Curran Associates, Inc., 2017. URL <http://papers.nips.cc/paper/6933-process-constrained-batch-bayesian-optimisation.pdf>.
- Zachary Wu, S. B. Jennifer Kan, Russell D. Lewis, Bruce J. Wittmann, and Frances H. Arnold. Machine learning-assisted directed protein evolution with combinatorial libraries. *Proceedings of the National Academy of Sciences*, 116(18):8852–8858, 2019. doi: 10.1073/pnas.1901979116. URL <https://doi.org/10.1073/pnas.1901979116>.
- Kevin K. Yang, Yuxin Chen, Alycia Lee, and Yisong Yue. Batched stochastic bayesian optimization via combinatorial constraints design. In Kamalika Chaudhuri and Masashi Sugiyama, editors, *Proceedings of Machine Learning Research*, volume 89 of *Proceedings of Machine Learning Research*, pages 3410–3419. PMLR, 16–18 Apr 2019. URL <http://proceedings.mlr.press/v89/yang19c.html>.
- Xiang Zheng, Xin-Hui Xing, and Chong Zhang. Targeted mutagenesis: a sniper-like diversity generator in microbial engineering. *Synthetic and Systems Biotechnology*, 2(2):75–86, 2017. doi: 10.1016/j.synbio.2017.07.001. URL <https://doi.org/10.1016/j.synbio.2017.07.001>.

A Appendix

A.1 Precursors

This section establishes generally useful properties for the following proofs. The proofs for discrete and continuous distributions are in regards to the cumulative expected regret at iteration T for each θ_t $1 \leq t \leq T$: $R_T = \sum_{i=1}^T r_\pi(\theta_t)$. For notational simplicity, we write r_t in place of $r_\pi(\theta_t)$.

Lemma 1. *Let x belong to a set D . Define σ_{t-1}^2 as the predictive variance of a GP with kernel $k(x, x) \leq 1$ and observation variance σ^2 trained on $t - 1$ observations. Then,*

$$\sum_{i=1}^T \frac{1}{2} \log(1 + \sigma^{-2} \sigma_{t-1}^2(x)) = I(Y_T; f)$$

Where Y_T corresponds to T observations selected by SS-GPUCB, and $I(Y_T; f)$ is the mutual information between observations Y_T and f .

Proof. The proof is adapted from [Srinivas et al., 2012], Lemma 5.3 but assuming a single $x \in D$. As we show below, our regret bounds can be stated with x held constant and the expectation taken over each θ_t . First, note that

$$I(Y_T; f) = H(Y_T) - H(Y_T|f).$$

We have, for a single observation y_T :

$$H(y_T|f) = \frac{1}{2} \log(2\pi e \sigma^2) \quad (18)$$

for all t because y_t given f is a normal variate. We also have

$$\begin{aligned} H(Y_T) &= H(Y_{T-1}) + H(y_T|Y_{T-1}) \\ &= H(Y_{T-1}) + \log(2\pi e(\sigma^2 + \sigma_{t-1}^2(x)))/2 \\ &= \frac{1}{2} \sum_{i=1}^T \log(2\pi e(\sigma^2 + \sigma_{t-1}^2(x))) \end{aligned}$$

The second equation follows from the fact that σ_{t-1}^2 does not depend on the values of Y_T . Finally we have

$$\begin{aligned} I(Y_T; f) &= \sum_{i=1}^T \left[\frac{1}{2} \log(2\pi e(\sigma^2 + \sigma_{t-1}^2(x))) - \frac{1}{2} \log(2\pi e \sigma^2) \right] \\ &= \sum_{i=1}^T \frac{1}{2} \log(1 + \sigma^{-2} \sigma_{t-1}^2(x)) \end{aligned}$$

□

From here we establish a useful bound on the sum of variance terms used in the following proofs.

Lemma 2. *Take a series over the variable t , $1 \leq t \leq T$. Suppose that the t dependent variable β_t is non-decreasing. Additionally, let there be an observation $x \in D$ for each iteration t . Let $\sigma_{t-1}(x)$ be the predictive variance at iteration $t - 1$ of a GP with kernel k such that $k(x, x) \leq 1$ for all x and noise variance σ^2 . Let $C_1 = \frac{8}{\log(1+\sigma^{-2})}$. Then,*

$$\sum_{t=1}^T 4\beta_t \sigma_{t-1}^2(x) \leq \beta_T \gamma_T C_1$$

Proof. First, we have

$$4\beta_t \sigma_{t-1}^2(x) \leq 4\beta_T \sigma_{t-1}^2(x)$$

because β_t is non-decreasing. Next,

$$\begin{aligned} 4\beta_T\sigma_{t-1}^2(x) &\leq 4\beta_T\sigma^2\sigma_{t-1}^2(x) \\ &\leq 4\beta_T\sigma^2C_2\log(1 + \sigma^{-2}\sigma_{t-1}(x)) \end{aligned}$$

where $C_2 = \frac{\sigma^{-2}}{\log(1+\sigma^{-2})}$. This is due to the fact that $s^2 \leq C_2 \log(1 + s^2)$ for $s^2 \in [0, \sigma^2]$ and $\sigma^{-2}\sigma_{t-1}^2(x) \leq \sigma^{-2}k(x, x) \leq \sigma^{-2}$. Then, due to the fact that $C_2 = \frac{C_1}{8\sigma^2}$, we have

$$4\beta_T\sigma^2C_2\log(1 + \sigma^{-2}\sigma_{t-1}(x)) \leq \beta_TC_1 \left[\frac{1}{2} \log(1 + \sigma^{-2}\sigma_{t-1}(x)) \right]$$

Therefore we have,

$$\sum_{t=1}^T 4\beta_t\sigma_{t-1}^2(x) \leq \beta_T\gamma_TC_1 \quad (19)$$

□

As described in the main text, for sampling distributions $\pi(x|\theta)$, we define a constant

$$\pi^* := \max_{x \in D, \theta \in \Theta} \pi(x|\theta).$$

π^* corresponds to the maximal pdf value of π for all possible x and θ in the optimization problem. This constant is useful for bounding the expected pdf value of π for a given θ , which arises in our proofs. Specifically,

$$E_{\pi(\theta)}[\pi(\theta)] = \sum_{x \in D} \pi^2(x|\theta) \leq \pi^* \sum_{x \in D} \pi(x|\theta) \leq \pi^* \quad (20)$$

for the discrete case, and

$$E_{\pi(\theta)}[\pi(\theta)] = \int \pi^2(x|\theta) dx \leq \pi^* \int \pi(x|\theta) dx \leq \pi^* \quad (21)$$

in the continuous case. Using these terms, we now state the main theoretical results of this work.

A.2 Discrete distribution

Here, we consider a sample space, and sampling distribution, with finite dimensionality. Specifically, $x \in D$ and $|D| < \infty$. Each sampling distribution is then well defined on this space, $\pi(x|\theta) > 0 \forall x \in D$ and $\sum_{x \in D} \pi(x|\theta) = 1 \forall \theta \in \Theta$. The proof for this case follows similarly to that of the finite dimensional case of the original GP-UCB paper [Srinivas et al., 2012].

Theorem A.1. *Let $\delta \in \{0, 1\}$ and $\beta_t = 2 \log(|D|\pi^2/6\delta)$. Then the regret associated with performing SS-GPUCB has the following probabilistic bound:*

$$Pr\left(R_T \leq \sqrt{TC_1\beta_T\gamma_T|D|\pi^*}\right) \geq 1 - \delta \quad (22)$$

Proof to follow.

Lemma 3 ([Srinivas et al., 2012] Lemma 5.1). *Pick $\delta \in (0, 1)$ and set $\beta_t = 2 \log(|D|\pi_t/\delta)$, such that $\sum_{t \geq 1} 1/\pi_t = 1$ and $\pi_t > 0$. Then,*

$$|f(x) - \mu_{t-1}(x)| \leq \beta_t^{1/2}\sigma_{t-1}(x) \quad \forall x \in D, \forall t \geq 1 \quad (23)$$

holds with probability $\geq 1 - \delta$.

Proof. See [Srinivas et al., 2012] Lemma 5.1. □

Lemma 4. *Fix $t \geq 1$. If $|f(x) - \mu_{t-1}(x)| \leq \beta_t^{1/2}\sigma_{t-1}(x)$ for all $x \in D$, then the expected regret $r_\pi(\theta_t) = \sum_{x \in D} f(x)\pi(x|\theta^*) - \sum_{x \in D} f(x)\pi(x|\theta_t)$ (Eq. 8) is bounded by $2\beta_t^{1/2}E_{\pi(x|\theta)}[\sigma_{t-1}(x)]$.*

Proof. The proof is similar to that of [Srinivas et al., 2012] Lemma 5.2, adapted to the expectation over $\pi(x|\theta)$. First, from the assumed bounds, we have for all $\theta \in \Theta$:

$$\sum_{x \in D} [f(x) - \mu_{t-1}(x)]\pi(x|\theta) \leq \sum_{x \in D} \beta^{1/2} \sigma_{t-1}(x) \pi(x|\theta).$$

and therefore

$$\sum_{x \in D} f(x)\pi(x|\theta) \leq \sum_{x \in D} [\mu_{t-1}(x) + \beta^{1/2} \sigma_{t-1}(x)]\pi(x|\theta) \quad (24)$$

$$\leq \sum_{x \in D} \alpha_t(x)\pi(x|\theta). \quad (25)$$

Then, by definition of θ_t (Eq. 9) and the above bounds, we have

$$\begin{aligned} \sum_{x \in D} f(x)\pi(x|\theta^*) &\leq \sum_{x \in D} \alpha_t(x)\pi(x|\theta^*) \\ &\leq \sum_{x \in D} \alpha_t(x)\pi(x|\theta_t) = E_{\pi(x|\theta_t)}[\alpha_t(x)] \end{aligned}$$

Therefore, we have

$$\begin{aligned} r_\pi(\theta_t) &= \sum_{x \in D} f(x)\pi(x|\theta^*) - \sum_{x \in D} f(x)\pi(x|\theta_t) \\ &\leq \sum_{x \in D} \alpha(x)\pi(x|\theta^*) - \sum_{x \in D} f(x)\pi(x|\theta_t) \\ &\leq \sum_{x \in D} \alpha(x)\pi(x|\theta_t) - \sum_{x \in D} f(x)\pi(x|\theta_t) \\ &\leq \sum_{x \in D} [\beta^{1/2} \sigma_{t-1}(x) + \mu_{t-1}(x) - f(x)]\pi(x|\theta_t) \\ &\leq \sum_{x \in D} 2\beta^{1/2} \sigma_{t-1}(x)\pi(x|\theta_t) \\ &\leq 2\beta^{1/2} E_{\pi(x|\theta_t)}[\sigma_{t-1}(x)]. \end{aligned}$$

□

Lemma 5. Set $\delta \in (0, 1)$ and β_t as above. Then the following holds with probability $1 - \delta$:

$$\sum_{t=1}^T (r_\pi(\theta_t))^2 \leq C_1 \beta_T \gamma_T |D| \pi^*.$$

Proof. From Lemma 4, we have:

$$\begin{aligned} \sum_{t=1}^T (r_\pi(\theta_t))^2 &\leq 4 \sum_{t=1}^T \beta_t E_{\pi(x|\theta_t)}^2[\sigma_{t-1}(x)] = 4 \sum_{t=1}^T \beta_t \left[\sum_{x \in D} \sigma_{t-1}(x)\pi(x|\theta_t) \right]^2 \\ &\leq 4 \sum_{t=1}^T \left(\beta_t \sum_{x \in D} \sigma_{t-1}^2(x) \sum_{x \in D} \pi^2(x|\theta_t) \right) \end{aligned}$$

where the second step comes from the Cauchy-Schwartz inequality. Using Eq. 20, we have

$$4 \sum_{t=1}^T \left(\beta_t \sum_{x \in D} \sigma_{t-1}^2(x) \sum_{x \in D} \pi^2(x|\theta_t) \right) \leq \pi^* \left(4 \sum_{t=1}^T \beta_t \sum_{x \in D} \sigma_{t-1}^2(x) \right).$$

Next we adapt the maximal information gain bound developed in [Srinivas et al., 2012]. Specifically, we have

$$\begin{aligned}
\sum_{t=1}^T 4\beta_t \sum_{x \in D} \sigma_{t-1}(x)^2 &= \sum_{x \in D} \sum_{t=1}^T 4\beta_t \sigma_{t-1}^2(x) \\
&\leq \sum_{x \in D} \beta_T C_1 I(y_T; f_T) \\
&\leq \sum_{x \in D} \beta_T C_1 \gamma_T \\
&\leq \beta_T C_1 \gamma_T |D|.
\end{aligned}$$

The first two steps follow those of Lemma 2. Combining terms we get the bounds as described. \square

From here, we use the fact that $R_T^2 \leq T \sum_{t=1}^T r_t^2$ from the Cauchy-Schwartz inequality to establish that $R_T \leq \sqrt{TC_1 \beta_T \gamma_T |D| \pi^*}$.

A.3 Continuous distribution

We now consider the case of closed, bounded $D \subset \mathbb{R}^d$. Specifically, we consider $D = [0, r]^d$, $d \in \mathbb{N}$ and $r > 0$. The volume of this set is then $V = r^d$.

Theorem A.2. *Let $D \subset [0, r]^d$ with $V = r^d$. Suppose that f is drawn from a GP with kernel k that satisfies the probability bound, for some constants $a, b > 0$:*

$$Pr\left(\sup_{x \in D} |\partial f / \partial x_j| > L\right) \leq ae^{-L^2/b^2} \quad j = 1, \dots, d.$$

Pick $\delta \in (0, 1)$ and set

$$\beta_t = 2 \log(t^2 2\pi^2 / (3\delta)) + 2d \log\left(t^2 dbr \sqrt{\log(4da/\delta)}\right).$$

Then

$$Pr\left(R_T \leq \sqrt{T\beta_T \gamma_T C_1 V \pi^*} + \pi^2/3\right) \geq 1 - \delta.$$

Proof to follow.

Lemma 6 (Adapted from [Srinivas et al., 2012] Lemma 5.5).

Let x_t be the point sampled at step t , given by $x_t \sim \pi(x|\theta_t)$. Choose $\delta \in (0, 1)$ and $\beta_t = 2 \log(\pi_t/\delta)$, with $\sum_{t \geq 1} \pi_t^{-1} = 1$ and $\pi_t > 0$. Then,

$$|f(x_t) - \mu_{t-1}(x_t)| \leq \beta_t^{1/2} \sigma_t(x_t) \quad \forall t \geq 1$$

holds with probability $1 - \delta$.

Proof. see [Srinivas et al., 2012] lemma 5.5. \square

For sake of analysis, define a discretization of D : $D_t \subset D$, $|D_t| < \infty$.

Lemma 7 (Adapted from [Srinivas et al., 2012] Lemma 5.6). *Pick $\delta \in (0, 1)$ and set $\beta_t = 2 \log(|D_t| \pi_t / \delta)$, with $\sum 1/\pi_t = 1$ and $\pi_t > 0$. Then,*

$$Pr\left(|f(x) - \mu_{t-1}(x)| \leq \beta_t \sigma_{t-1}(x) \quad \forall x \in D_t, \forall t \geq 1\right) \geq 1 - \delta.$$

Proof. Same as Lemma 3, replacing finite D with D_t . \square

Now assume that

$$Pr(\forall j, \forall x \in D, |\partial f / \partial x_j| < L) \geq 1 - da \exp(-L^2/b^2).$$

From which follows

$$Pr(\forall x, x' \in D, |f(x) - f(x')| < L \|x - x'\|_1) \geq 1 - da \exp(-L^2/b^2). \quad (26)$$

Next, set the size of D_t to τ_t^d such that for all $x \in D$,

$$\|x - [x]_t\|_1 \leq rd/\tau_t,$$

where $[x]_t$ corresponds to the closest point in D_t to x . This can be accomplished by placing τ_t equally spaced coordinates in each dimension.

Lemma 8 (Adapted from [Srinivas et al., 2012] Lemma 5.7). *Pick $\delta \in (0, 1)$ and set $\beta_t = 2 \log(2\pi_t/\delta) + 4d \log(dtbr\sqrt{\log(2da/\delta)})$ where $\sum \pi_t^{-1} = 1$ and $\pi_t > 0$. Let $\tau_t = dt^2br\sqrt{\log(2da/\delta)}$. Then*

$$Pr(|f(x) - \mu_t([x]_t)| \leq \beta_t^{1/2} \sigma_t([x]_t) + \frac{1}{t^2}; \forall t, \forall x \in D) > 1 - \delta. \quad (27)$$

Proof. From Eq. 26 we have

$$Pr(\forall x, x' \in D |f(x) - f(x')| \leq b\sqrt{\log(2da/\delta)} \|x - x'\|_1) \geq 1 - \delta/2.$$

Then,

$$Pr(|f(x) - f([x]_t)| \leq \frac{rd}{\tau_t} b\sqrt{\log(2da/\delta)}) \geq 1 - \delta/2.$$

Therefore, with the selected value of τ_t , we have

$$Pr(|f(x) - f([x]_t)| \leq \frac{1}{t^2}; \forall x \in D) \geq 1 - \delta/2.$$

With the specified value of τ_t , we have $|D_t| = (dt^2br\sqrt{\log(2da/\delta)})^d$. Then, with probability $\delta/2$ substituted into Lemma 7, the result follows as described. \square

In order to minimize the expected regret, we now adapt the UCB calculation to marginalize within the set D_t . Specifically, find θ_t as

$$\theta_t := \arg \max_{\theta \in \Theta} \int \alpha([x]_t) \pi(x|\theta) dx.$$

First, from this definition of θ_t and the previous lemma we have with probability $\geq 1 - \delta$,

$$\begin{aligned} \int f(x) \pi(x|\theta^*) dx &\leq \int \left(\mu_t([x]_t) + \beta_t^{1/2} \sigma_t([x]_t) + \frac{1}{t^2} \right) \pi(x|\theta^*) dx \\ &\leq \int \left(\alpha([x]_t) + \frac{1}{t^2} \right) \pi(x|\theta^*) dx \\ &\leq \int \left(\alpha([x]_t) + \frac{1}{t^2} \right) \pi(x|\theta_t) dx \\ &\leq \int \left(\mu_t([x]_t) + \beta_t^{1/2} \sigma_t([x]_t) + \frac{1}{t^2} \right) \pi(x|\theta_t) dx. \end{aligned}$$

Then, we have

$$\begin{aligned} r_\pi(\theta_t) &= \int f(x) \pi(x|\theta^*) dx - \int f(x) \pi(x|\theta_t) dx \\ &\leq \int \left(\beta_t^{1/2} \sigma_t([x]_t) + \mu_t([x]_t) - f(x) + \frac{1}{t^2} \right) \pi(x|\theta_t) dx \\ &\leq \int \left(2\beta_t^{1/2} \sigma_t([x]_t) + 2\frac{1}{t^2} \right) \pi(x|\theta_t) dx \\ &\leq \frac{2}{t^2} + \int 2\beta_t^{1/2} \sigma_t([x]_t) \pi(x|\theta_t) dx \end{aligned}$$

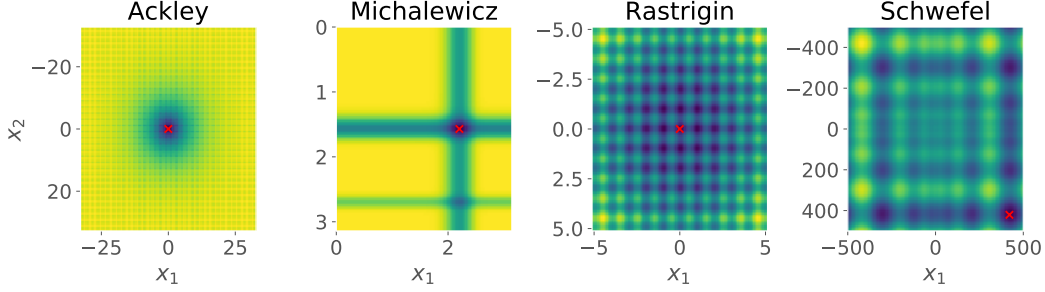


Figure A.1: **Objective functions used for simulations.** 2-dimensional views of the objective functions used in this study. These functions were taken from standard bench-marking literature on optimization processes. These objectives have various useful properties for assessing optimization techniques, including local optima, multiple periodicities and magnitudes, and sharp boundaries.

Table A.1: Objective functions. $d = 2$ in all cases.

Function	Equation	range
Ackley	$-20\exp\left(-0.2\sqrt{\frac{1}{d}\sum_{i=1}^d x_i^2}\right) - \exp\left(\frac{1}{d}\sum_{i=1}^d \cos(2\pi x_i)\right) + 20 + \exp(1)$	$-32.768 \leq x \leq 32.768$
Michaelwicz	$-\sum_{i=1}^d \sin(x_i)\sin^{2m}\left(\frac{ix_i^2}{\pi}\right)$	$0 \leq x \leq \pi$
Rastrigin	$10d + \sum_{i=1}^d (x_i^2 - 10\cos(2\pi x_i))$	$-5.12 \leq x \leq 5.12$
Schwefel	$418.9829d - \sum_{i=1}^d x_i \sin(\sqrt{ x_i })$	$-500 \leq x \leq 500$

Then, bound the second term similar to lemma 4 for the discrete case using the Cauchy-Schwartz inequality. First, we have

$$\sum_{i=1}^T \left(\int (2\beta^{1/2}\sigma_t([x]_t))\pi(x|\theta_t)dx \right)^2 \leq \sum_{i=1}^T \int (4\beta\sigma_t^2([x]_t))dx \int \pi^2(x|\theta_t)dx \quad \text{via Cauchy-Schwartz} \quad (28)$$

$$\leq \pi^* \sum_{i=1}^T \int (4\beta\sigma_t^2([x]_t))dx \quad \text{via Eq. 21} \quad (29)$$

$$\leq \pi^* \int \sum_{i=1}^T (4\beta\sigma_t^2([x]_t))dx \quad (30)$$

$$\leq \pi^* V\beta_T\gamma_T C_1 \quad (31)$$

Returning to the expected regret, we have

$$R_T = \sum_{t=1}^T r_\pi(\theta_t) = \sum_{i=1}^T \left(\int (2\beta^{1/2}\sigma_t([x]_t))\pi(x|\theta_t)dx \right) + \pi^2/3 \quad \text{because } \sum 1/t^2 = \pi^2/6$$

$$\leq \sqrt{T\beta_T\gamma_T C_1 V\pi^*} + \pi^2/3 \quad \text{via Eq. 31 and Cauchy-Schwartz}$$

A.4 Exact marginalization of acquisition function

As in [Desautels et al. \[2014\]](#), define a feedback function $\text{fb}[t]$ specifying the number of observations available at iteration t . For example, if each batch is of fixed size B , then $\text{fb}[t] = \lfloor (t-1)/B \rfloor B$. Normal sequential feedback corresponds to $\text{fb}[t] = t-1$. Define

$$\hat{\alpha}_t(x) = \mu_{\text{fb}[t]}(x) + \beta^{1/2}\sigma_{t-1}(x), \quad (32)$$

be the approximation of $\alpha_t(x)$ as suggested in [\[Desautels et al., 2014\]](#). The predictive mean is computed from the available feedback at a given iteration t (e.g. $\text{fb}[t]$ data points) while $\sigma_t(x)$ can be calculated exactly because it does not depend on the observations.

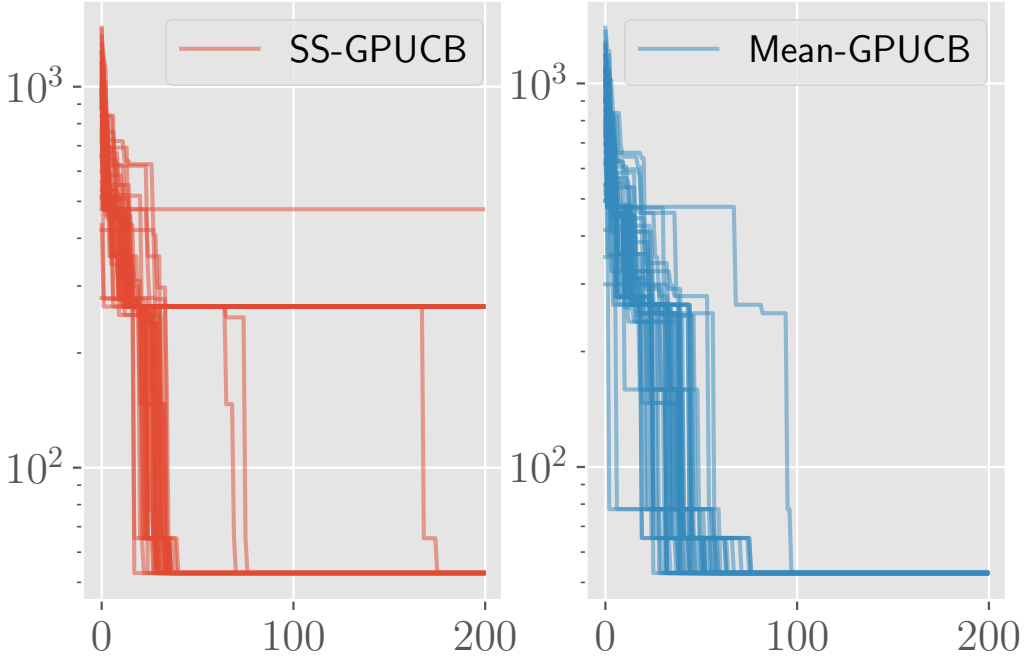


Figure A.2: **Simple regret trace plots for Schwefel function.** Simple regret trace plots for sequential stochastic optimization for SS-GPUCB and Mean-GPUCB

At time t , define the expected UCB for a batch of size B as

$$E_{\pi(\theta)} \left[\sum_{i=1}^B \alpha_{t+i}(x) \right] = \sum_{i=1}^B E_{\pi(\theta)} [\alpha_{t+i}(x) | x_{1:t+i-1}] \quad (33)$$

$$\approx \sum_{i=1}^B E_{\pi(\theta)} [\hat{\alpha}_{t+i}(x) | x_{1:t+i-1}], \quad (34)$$

where $x_{1:t+i-1} = \{x_1, \dots, x_{t+i-1}\}$ are the location of observations 1 to $t+i-1$. The issue with this calculation arises from the term $\sigma_{t-1}(x)$ in $\hat{\alpha}_t(x)$. This term depends on previous observations in the batch $x_{t:t+i-1}$ and therefore requires an expectation calculation over the inverse of the kernel matrix including these terms. For exact calculation, this requires a combinatorial calculation for each possible x_i , $t \leq i \leq t+i-1$. Alternatively, Monte-carlo methods can be employed [Snoek et al., 2012].

A.5 Batch penalty calculation

We use the local penalty calculation of [González et al., 2015], which is constructed with the assumption of Lipschitz continuity on the optimization target f . Specifically there is some L such that

$$|f(x_1) - f(x_2)| \leq L \|x_1 - x_2\|, \quad \forall x_1, x_2 \in D. \quad (35)$$

This constant is estimated from the current model as

$$\hat{L} = \max_{x \in D, i \in k} \left\| \frac{d}{dx^{(i)}} \mu(x) \right\|, \quad (36)$$

where $\frac{d}{dx^{(i)}}$ is the derivative with respect to input dimension i as is directly calculated from the GP model [Solak et al., 2003]. This term is then combined with \hat{M} , the approximate maximum of the function calculated from all current observations, the local penalty function $\varphi(x_j; x_k)$ for previously

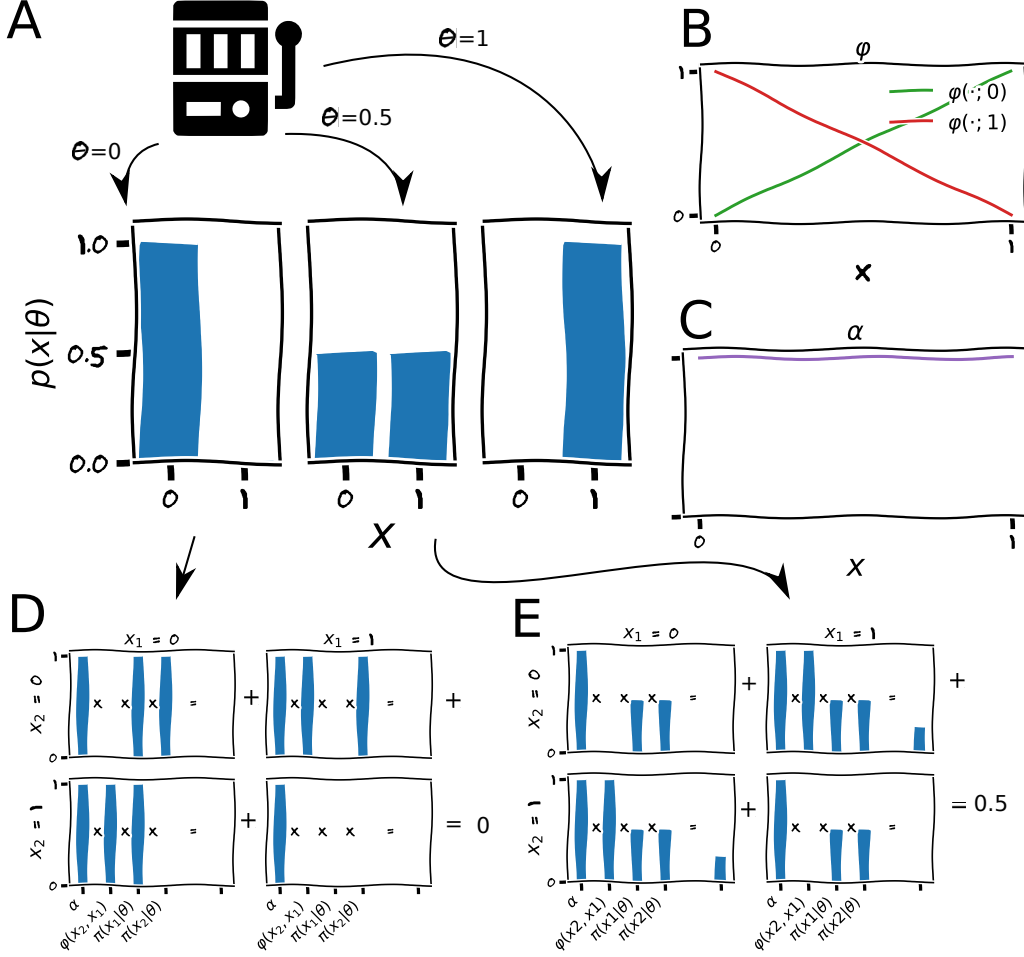


Figure A.3: **Simplified example of batch penalty usage.** A simple three armed bandit (A) with parameter space $\Theta = \{0, .5, 1\}$. We consider the acquisition value for each possible θ when sampling two values x_1 and x_2 . We simplify the acquisition penalty function φ to be 1 when the two x values differ and 0, otherwise (B). We also assume no previous data exists for this model, so the acquisition for both outcomes of x are equal (C). The total acquisition value for a specific θ is the expected acquisition of both x_1 and x_2 : $E_{\pi(\theta)}[\alpha(x_1) + \alpha(x_2)\varphi(x_2; x_1)]$. The first term simplifies to 1 for each value of θ but the second term must be evaluated for each pair of x_1 and x_2 (D,E). For $\theta = 0$, there is no non-zero term in this portion of the expectation (D). For $\theta = 0.5$ however, the case where x_1 and x_2 differ occurs 50 % of the time, leading to a total acquisition value of 0.5 from the second sample in the batch (E). In total, the acquisition for $\theta = 0$ (or = 1) is 1 while for $\theta = 0.5$ it is 1.5. Therefore, applying the penalty φ allows the algorithm to properly weight the overlap in information between repeated sampling from the same distribution $\pi(\theta)$.

selected observation position x_k is

$$\varphi(x_j; x_k) = \frac{1}{2} \operatorname{erfc} \left(-\frac{\hat{L} \|x_j - x_k\| - \hat{M} + \mu_n(x_j)}{\sqrt{2\sigma_n^2(x_j)}} \right), \quad (37)$$

where erfc is the complementary error function, and $\mu_n(\cdot)$ and $\sigma_n^2(\cdot)$ are the predictive mean and variance respectively of the GP model at iteration n .

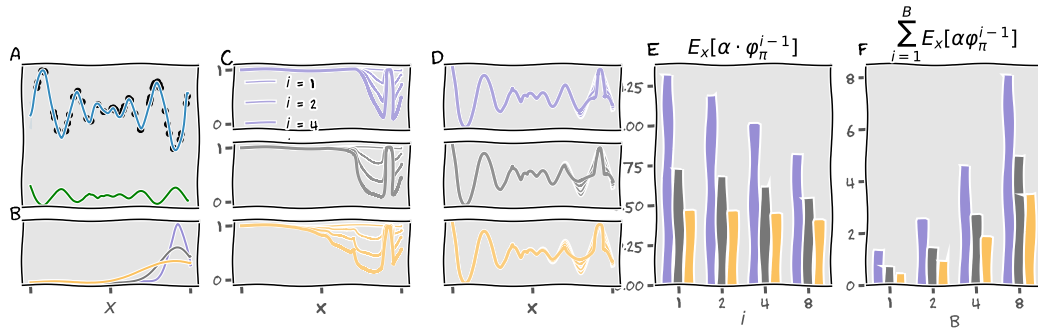


Figure A.4: **Batch penalty calculations during late iterations.** (A) GP model (blue) during late-stage optimization (e.g. many observations) and acquisition function (green). (B) Sampling distributions. (C) Expected penalty φ for each sampling distribution and varying iteration i . (D) Expected acquisition penalized by φ for each distribution and varying iteration i . (E) Expected acquisition for iteration i and (F) batch size B .

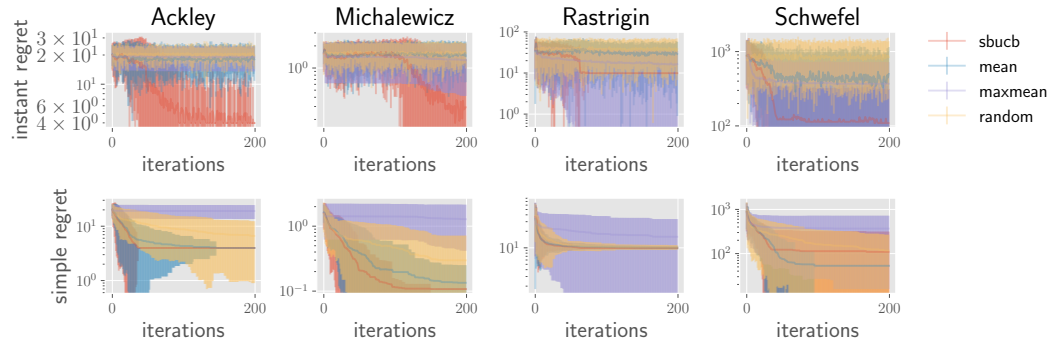


Figure A.5: **Error on sequential regret.** 95 % interval of regret for sequential optimization.

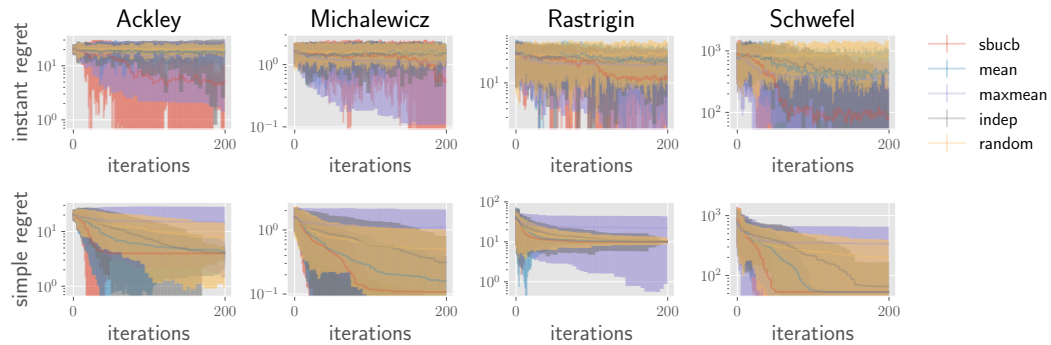


Figure A.6: **Error on batch regret** 95 % interval of regret for batch optimization.

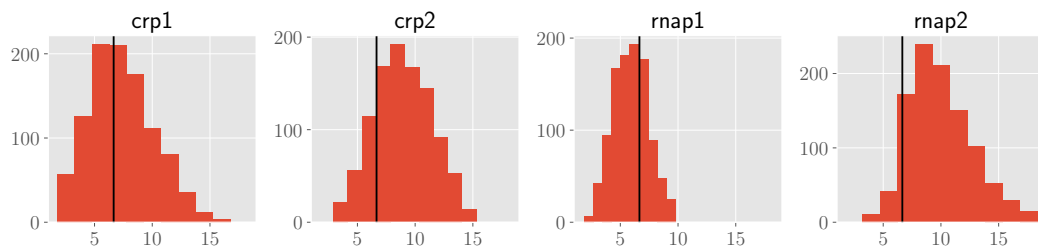


Figure A.7: **Distribution of LacI promoter fitness for various randomized regions.** Distribution of fitness values for each promoter region. Black line is wild-type fitness.

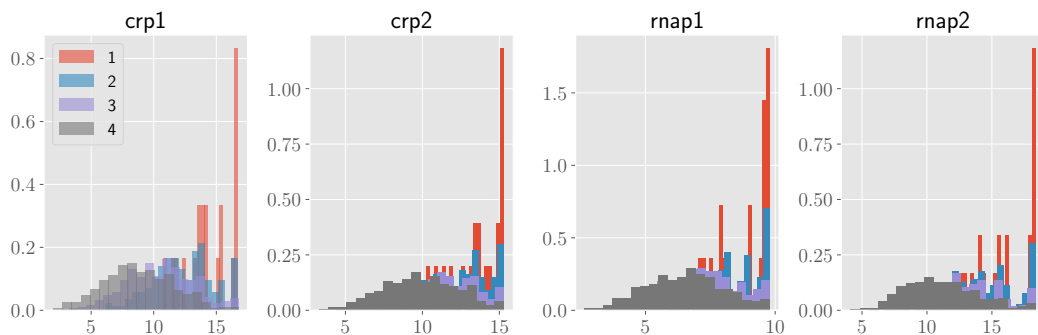


Figure A.8: **Local optima landscape** Local fitness landscape for each promoter region. The distribution of fitness values with hamming distance (1—4) from the optima.

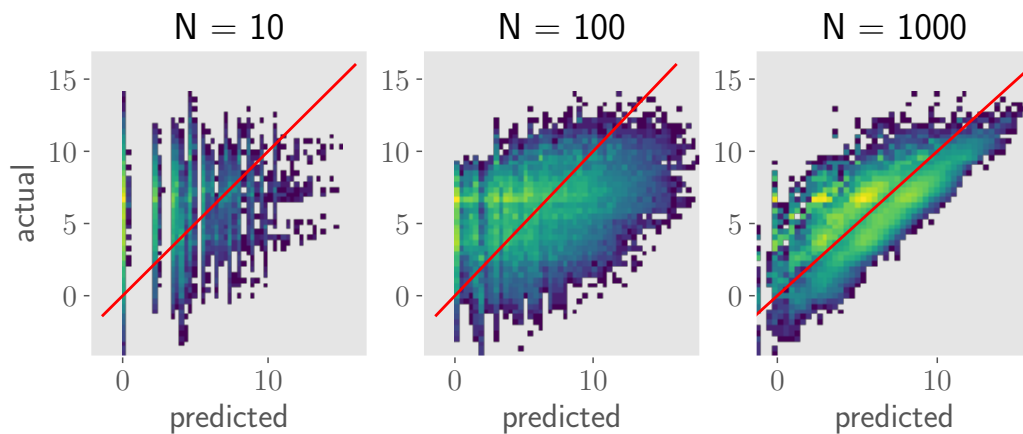


Figure A.9: **GP model prediction of LacI binding for increasing sample size.** GP model predictive mean vs actual fitness for models trained with varying sample size.